11th World Congress on Computational Mechanics (WCCM XI)
5th European Conference on Computational Mechanics (ECCM V)
6th European Conference on Computational Fluid Dynamics (ECFD VI)
E. Oñate, J. Oliver and A. Huerta (Eds)

3D CFD ANALYSIS OF A TWIN SCREW EXPANDER FOR SMALL SCALE ORC SYSTEMS

IVA PAPES, JORIS DEGROOTE AND JAN VIERENDEELS

Ghent University
Department for Flow, Heat and Combustion Mechanics
e-mail: iva.papes@ugent.be

Key words: Screw expander, R245fa, ORC, Redlich-Kwong, real gas

Abstract. Among a number of solutions to generate electricity from low temperature heat sources, the Organic Rankine Cycle (ORC) is the most widely used. In small scale ORC systems (below 300 kWe) with a low temperature heat source (from 55°C till 150°C), twin screw expanders are commonly used to recover the mechanical power. In this paper, 3D CFD (Computational Fluid Dynamics) calculations of a twin screw expander, with R245fa as a working fluid, are performed. The mesh motion is handled by an in-house code which generates a block-structured grid with the help of solutions of Laplace problems. Since the ideal gas equation of state shows big deviations in the ORC working conditions, the cubic Aungier Redlich-Kwong equation of state has been used because of its relative simplicity and low computational cost.

The performance of the expander is evaluated for different pressure ratios and for two different designs. It is observed that the leakage flows have a significant effect on the screw expander's efficiency. In order to evaluate the effects of individual clearance gaps on the performance of the expander, diagrams with the mass flow rate as a function of the rotation angle are provided.

1 INTRODUCTION

With the growing energy demand and the pollution produced by the combustion of fossil fuels, the interest to generate electricity from renewable sources like waste heat has dramatically grown. This waste heat is usually discarded but now it can be recovered to produce useful energy. Although the conventional methods for energy recovery in an industrial process are economically infeasible due to the low temperature of the heat source, the solution is the Organic Rankine Cycle (ORC). The ORC is named for its use of an organic, high molecular mass fluid (instead of water) which is characterized by low saturation temperatures. Although these ORC systems are now well developed, research efforts are increasingly directed towards higher efficiencies and powers.

Expanders for the organic fluids are the key element for power generation in the ORC systems. Studies have shown a big potential of positive displacement machines, like a twin screw expander, for small scale ORC systems [1]. One of the advantages of using screw expanders is the possibility to use existing compressors with opposite sense of rotation.

In Computational Fluid Dynamics (CFD) analysis of positive displacement machines, such as screw expanders, only a time-dependent (unsteady) simulation is meaningful. The rotor surfaces (which are boundaries of the flow problem) move in a complex manner and therefore a powerful grid manipulator is necessary for CFD calculations. In this paper an in-house code presented in [2] is used. The validation of the grid generator for a twin screw compressor has been reported in [3]. Since the validation showed good agreement between the experimental results and CFD calculations, the same procedure is used for the expander's simulations where only the sense of rotation is changed.

Different mathematical models have been constructed in [4, 5, 6] to estimate the leakage flows. Recently, the influence of the clearance sizes on the performance of the screw expander has been investigated by means of CFD calculations in [7]. Despite these investigations, the mass through the clearance as a function of the rotation angle are still lacking in the literature. Consequently, an effort was directed towards this study.

The screw expander used in the simulations was originally used as an oil-injected twin screw compressor. With the special wear-protection coating on the profiled part of the rotors and use of timing gears, this machine can be used as a oil-free screw expander.

The screw expanders are characterized by a fixed built-in volume ratio v, determined by the form of the inlet and outlet surfaces. This built-in volume ratio determines the internal pressure ratio by $\pi = v^k$ [8], where k is specific heat ratio for the selected fluid. For the best performance, the built-in volume ratio should match the operating conditions in order to limit the over- and under-expansion losses. If the internal volume ratio is too high for a given set of operating conditions, the fluid remains trapped longer than necessary, leading to a pressure drop below the discharge pressure (over-expansion). On the contrary, if the internal volume ratio is too low, the fluid in the chamber remains above the discharge pressure when the discharge/outlet port starts to open (under-expansion). Therefore, depending on the imposed internal pressure ratio, under- or over-expansion losses can decrease the efficiency of the screw expander.

Apart from over- and under-expansion, the efficiency of the screw expander is mainly governed by the leakage flows through the clearances and suction pressure losses. Depending on the internal pressure ratio, leakage flows from adjacent chambers can cause re-filling and consequently, affect the volumetric efficiency of the expander [7]. On the other hand, during the suction, inlet throttling occurs because the inlet surface is blocked by the tips of the rotor and the filling is reduced, which will decrease the volumetric efficiency.

In this paper, the performance of a screw expander is studied for different pressure ratios and for two different expander designs. The difference between these two designs are additional injection ports. The leakage flows inside the screw expander and the suction

losses are described. Based on this study, better expander design can be designed.

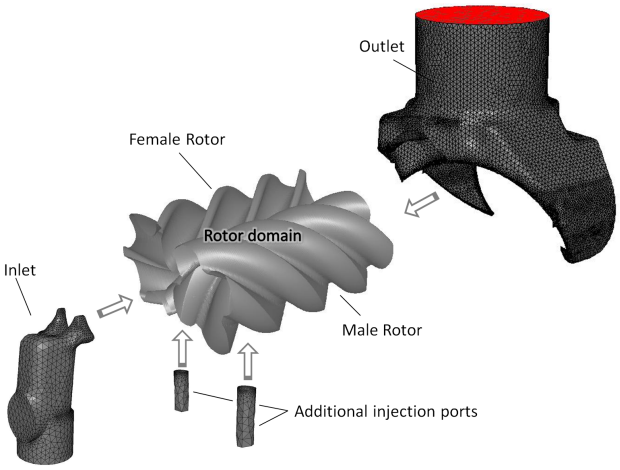

Figure 1: The geometry of the twin screw expander, with different parts shown separately for clarity

2 CFD ANALYSIS

The geometry of the twin screw expander is shown in Fig. 1. The grid in the inlet, outlet and oil injection ports is stationary (tetrahedral cells) and therefore is not handled by the grid generation algorithm mentioned in the introduction.

2.1 Grid generation in the rotor domain

The grid in the casing is built by stacking two-dimensional structured (rectangular) grids in slices of the casing (Fig. 2). Before the CFD simulation, 2D structured meshes are constructed in slices corresponding with different rotation of profiles, with step of 1.5 degrees of male rotor. These 2D meshes are generated using Laplace potential equation $\bigtriangledown^2\phi = 0$ as described in [2]. During the entire simulation the cells definitions are the same (the same faces and nodes). So, the nodes of the grid are moved in the housing (ALE, Arbitrary Langrangian-Eulerian method). For each time step in the calculation, a new position of the grid nodes can be found by interpolating between two supplied grids.

The size of the gaps between the rotors and between the rotors and the casing are extremely small (order tens of microns versus rotor diameter of about 70 mm). To reach sufficient numerical accuracy, the number of cells in radial direction is set to 8 (zoomed view in Fig. 2).

All blocks are joined together by using sliding interfaces between the inlet, outlet, the injection ports and the casing. The complete 3D mesh of the twin screw expander consists of 2060515 cells.

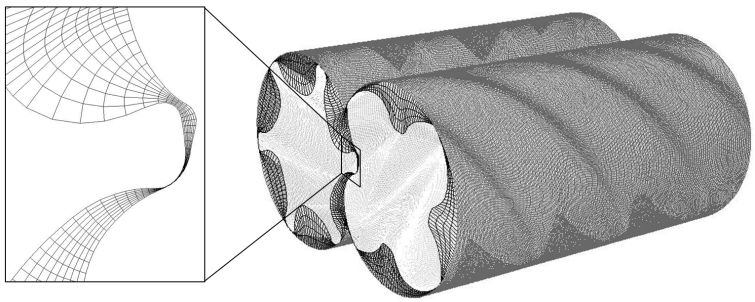

Figure 2: Grid in rotor domain

2.2 Geometrical parameters

The configuration of the rotor lobes is 4/6 (male/female). The outer diameter of the male and female rotors is approximately 70 mm with the L/D ratio is 1.86. The volume curve of the screw expander is shown in Fig. 3. The formation of a chamber starts when the male and female lobes are in connection with the inlet port (zero degrees in Fig. 3). As the rotors rotate, the volume of the chamber is rising together with the increase in inlet surface area. But, it is only for a short time that the surface of the inlet port is completely available for the filling (zoomed view in Fig. 3). Since a significant pressure drop occurs during the filling (Section 3.1.), the inlet port should be designed in a such way that filling occurs only during a small part of the growing phase of the volume with maximum inlet surface area available.

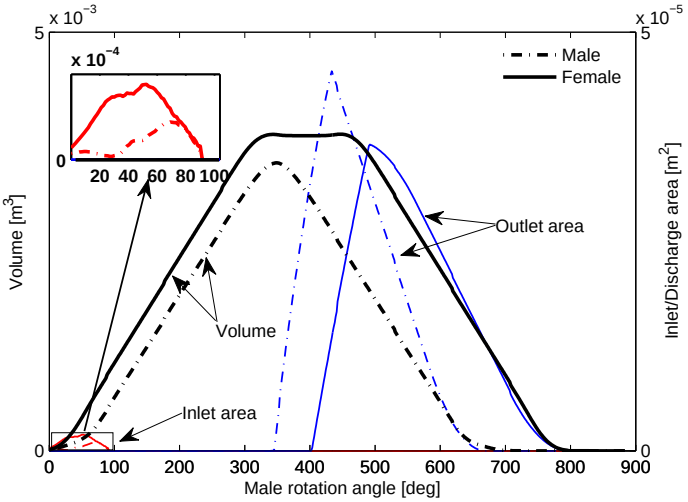

Figure 3: Volume curve with inlet and outlet surface area as a function of the rotational angle of the male rotor

2.3 Simulation parameters

The fluid flow inside the screw expander is compressible and is described by the set of momentum, energy and mass conservation equations, which are accompanied by the equation of state and the $k-\varepsilon$ turbulence model. The governing differential equations are solved by a commercial package with use of user-defined functions to handle the grid movement and real gas behaviour.

In ORC systems with a low temperature heat source, R245fa is one of the most commonly used organic fluids. Since the ideal gas equation of state shows big deviations in the ORC working conditions [9], an appropriate real gas equation of state should be used. In this paper the Aungier Redlich-Kwong equation of state is used [10]. It represents a modified form of the Redlich-Kwong equation of state. This new correlation includes an acentric factor and the critical point compressibility factor as additional parameters to improve its accuracy. The Aungier Redlich-Kwong equation of state is defined with the following equations:

$$
\begin{aligned}
&P = \frac{RT}{(V-\tilde{b})} - \frac{a(T)}{V(V+b_0)} \\
&Where: \\
&a(T) = a_0(\frac{T_c}{T})^n, a_0 = 0.42747\frac{R^2T_c^2}{p_c} \\
&b_0 = 0.08664\frac{RT_c}{p_c}, c_0 = \frac{RT_c}{p_c + \frac{a_0}{V_c(V_c+b_0)}} + b_0 - V_c, \tilde{b} = b_0 - c_0
\end{aligned}
\tag{1}
$$

In these equations, P is the pressure, T is the temperature, V is the specific volume and R is a gas constant. The subscript c in the above equations, refers to the critical value. However, it is important that the flow conditions in every cell are always in the gas phase region. If they fall outside that region, the partial derivative of pressure at constant temperature with respect to specific volume becomes positive. Since the rotor motion is complex and the volume of some cells can be extremely small (gap region), this can cause convergence problems during the start up. Therefore, the Aungier modified form was implemented in the commercial solver through user-defined functions with additional limiting functions. These limiting functions are disabled after the start-up period, when the flow reaches a periodic regime.

During the numerical simulation, the following operating conditions were selected: rotation speed $n = 6000rpm$ for the male rotor, outlet pressure $p_{out} = 1bar$, inlet temperature of the working fluid $\vartheta_{in} = 126.5°\mathrm{C}$. The effects of a variation in the pressure ratio are then studied.

The spatial discretization that is used for the calculations is first-order upwind. The temporal discretization is first-order implicit. The solver calculates the pressure and velocity simultaneously.

3 PERFORMANCE ANALYSIS AND RESULTS

In this paper, two expander designs are studied, with and without additional injection ports. The performance analysis is done for both configurations in order to indicate how its design might be altered to achieve better performance. The design with additional injection ports can also be used for the oil-injected twin screw expander where working fluid is mixed with a small percentage of oil.

During the simulation run, the mass flow rate (MFR) and the generated power of the twin screw expander are monitored. In Table 1, the mass flow rates and the generated power are averaged over one period (360 degrees male rotation) which corresponds with 4 expansion cycles.

Table 1: Cases evaluated for expander with and without additional injection ports

Inlet pressure *bar*	**Inlet MFR** *kg/s*	**Injection MFR** *kg/s*	**Power** *kW*
Additional injection ports			
6	0.171	0.145	7.14
5	0.140	0.115	5.40
4	0.111	0.087	3.69
3	0.082	0.057	1.94
2	0.053	0.022	0.06
Without injection ports			
6	0.174	0	4.72
5	0.142	0	3.46
4	0.111	0	2.18

3.1 Pressure-Volume Diagram

P-V diagrams for cases of the inlet pressure between $p_{in} = 6bar$ and $p_{in} = 2bar$ for both designs are presented in Fig. 4 and Fig. 5. In both figures, only a female working chamber is represented, since the pressure in the corresponding male chamber is the same. In the P-V diagram, the following phases can be distinguished:

- **Filling process**: Looking from the high pressure side, fluid starts to fill an expanding chamber formed between the lobes of the rotor profiles and the casing of the expander. Since it is only for a short time that the inlet is completely open for working fluid to enter the working chamber (Fig. 1), throttling losses and a pressure drop will occur (first pressure drop in a P-V diagram). Closing of the inlet (decrease in inlet surface area) in connection with the increase in volume of the chamber will cause the so called pre-

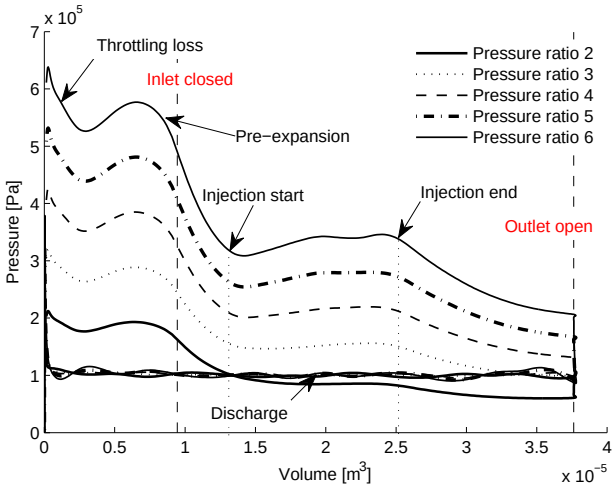

Figure 4: P-V diagram of the expansion for different pressure ratios (design with additional injection ports)

expansion (second pressure drop in a P-V diagram).

- **Expansion**: Once the chamber is disconnected from the inlet, the volume increases until the maximum volume is reached. Addition of working fluid through the injection ports will cause an increase in pressure in a chamber, despite it's increasing volume. This will however affect the slope of the P-V curve.

- **Discharge**: As the chamber meets the outlet port, the fluid in the chamber is discharged. Depending on the imposed pressure ratio, over- or under-expansion can be seen.

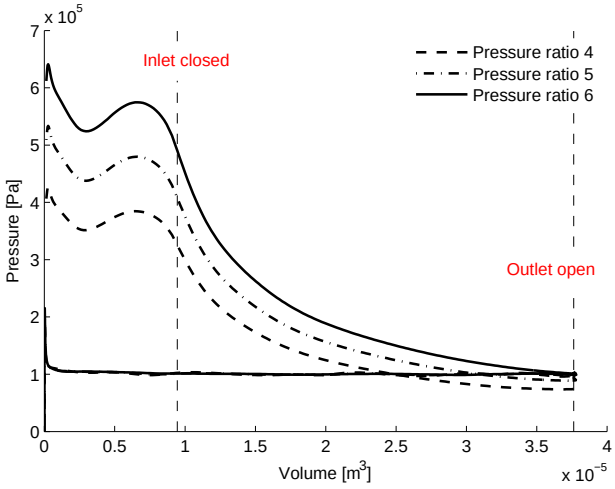

Figure 5: P-V diagram of the expansion for different pressure ratios (design without additional injection ports)

Comparing Fig. 4 and Fig. 5, it can be seen that with additional injection of the working fluid, the slope of the P-V curve can be changed in a way that it overcomes the over- and under-expansion losses. Looking at the area under the P-V diagram (indicated power) it can be concluded that the design with additional injection ports will generate more power. The generated power calculated from the CFD calculations (torque on the rotors walls multiplied by rotational speed) is presented in Table 1.

3.2 Mass Flow Rates

In Fig. 6, the mass flow rates through inlet and outlet ports are shown for 360 degrees of male rotation. In Fig. 6 (b), the influence of the over- and under- expansion on the mass flow rate is shown. For pressure ratio 2, there is reversed flow at the outlet during a fraction of each cycle.

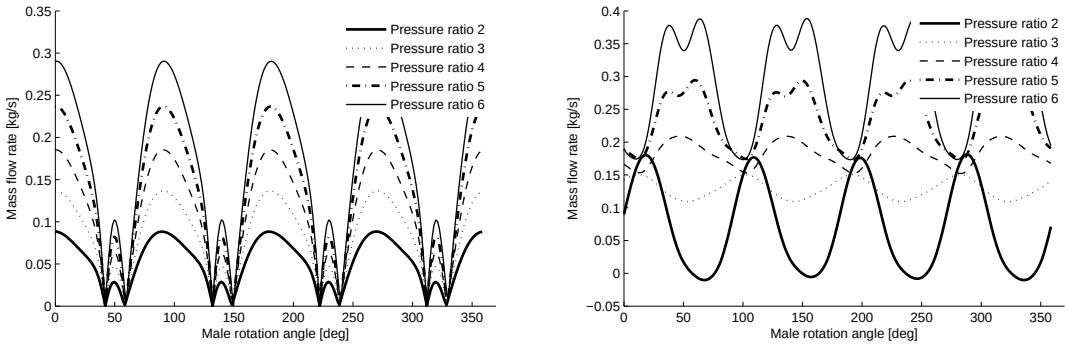

Figure 6: Mass flow rate at the inlet (a) and outlet (b) for different pressure ratios (design with additional injection ports)

3.3 Internal Leakages

In this paper special focus is on the study of leakage flows. These leakage flows have a very large impact on the expander's efficiency. Therefore, it is paramount that these leakage flows are assessed correctly. In the screw compressor/expander there are four types of gap clearances where leakages occur:

-**Tips**, the clearances between the rotor and the housing, which allow leakage flows from a working chamber to another chamber at a lower pressure.

-**Sealing**, the clearance between the meshing rotors. The sealing line can be defined as the line along which the rotors seal the fluid between high and low pressure areas.

-**Blowholes**, triangular gaps that are formed at the cusps between two rotors. Because of manufacturing reasons, it is impossible to have a sealing line that reaches to the cusp

of the housing.

-**End planes**, the clearances on the inlet and outlet side of the expander.

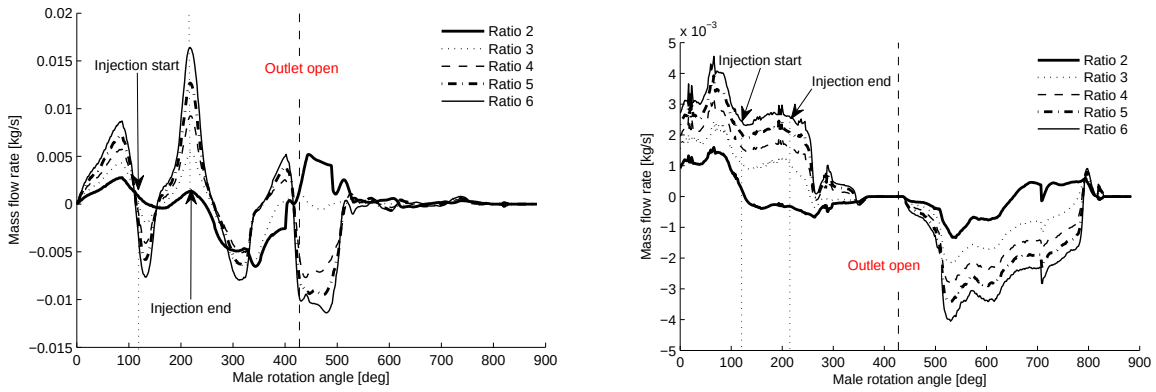

(a) (b)

Figure 7: Leakage flows through (a) tip and (b) sealing clearance gaps (design with additional injection ports)

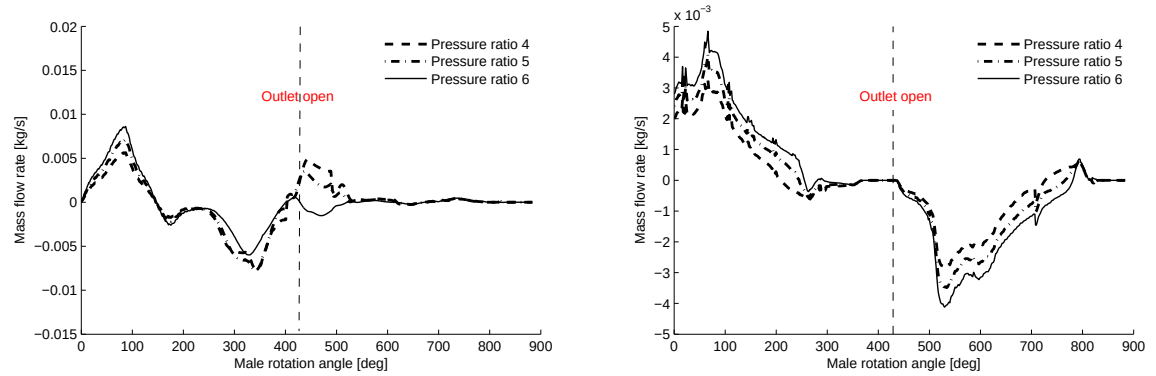

(a) (b)

Figure 8: Leakage flows through (a) tip and (b) sealing clearance gaps (design without additional injection ports)

In this paper we focus only on tip and sealing leakage flows. With an increase in pressure ratio, the internal leakage flows are rising, as depicted in Fig. 7 and Fig. 8. In these figures, a positive value means that the flow is leaving the current chamber. During the filling (until 80 degrees of male rotation), the outflows via both leakage paths are rising. During the expansion, the inflow through clearances increases, since the pressure

in an adjacent chamber (which in this moment is connected with the inlet) is higher. If in this moment, additional working fluid is injected through injection ports (Fig. 7(a)), the outflow through clearances will increase. After the chamber is connected with the outlet, two cases are possible. In the case of high pressure ratios (between $p_{in} = 6bar$ and $p_{in} = 3bar$), the inflow is dominating (since the pressure in the adjacent chamber is still much higher than at the outlet port). In the case of over-expansion with imposed pressure of $p_{in} = 2bar$ at the inlet, the outflow will increase (since the pressure in the adjacent chamber is lower than pressure at the outlet port).

4 CONCLUSION

In this paper, transient 3D CFD calculations of a twin screw expander with R245fa as a working fluid are carried out. The calculations are performed with the use of a grid manipulation algorithm and a commercial CFD solver accompanied by user-defined functions. From the results of the CFD calculations it can be seen where the pressure drops occur. With additional injection ports and for certain pressure ratios, the over-expansion can be avoided comparing to the design without injection ports. It is also shown that with the additional injection of the working fluid, the generated power increased. For the first time, leakage flows as a function of rotation angle of male rotor are presented and analysed.

REFERENCES

[1] Smith, I.K. and Stosic, N. *Cost effective small scale ORC systems for power recovery from low grade heat sources*. Proceedings of ASME International Mechanical Engineering Congress and Exposition, Chicago, Illinois, USA, pp. 1-7, 2006.

[2] Vande Voorde, J., Vierendeels, J. and Dick, E. *Development of a Laplacian-based mesh generator for ALE calculations in rotary volumetric pumps and compressors* Computer Methods in Applied Mechanics and Engineering, Vol. 193, 39-41, pp. 4401-4415, 2004.

[3] Vande Voorde, J., Vierendeels, J. and Dick, E. *ALE Calculations of Flow Through Rotary Positive Displacement Machines* In Proc. of the ASME Fluids Engineering Divison Summer Meeting and Exhibition, FEDSM2005-77353, ISBN 0-7918-3760-2,Huston, USA, June 19-23 2005.

[4] Seshaiah, N. and Ghosh, S.K. and Sahoo, R.K. and Sarangi, S.K. *Performance Analysis of Oil Injected Twin Screw Compressor* 18th National and 7th ISHMT-ASME Heat and Mass Transfer Conference, India, 2006.

[5] Lemort, V. and Quoilin, S. *Designing scroll expanders for use in heat recovery Rankine cycles*, Proc. of the IMechE, London, 2009.

[6] Fujiwara, M. and Osada, Y. *Performance analysis of an oil-injected screw compressor and its application* International Journal of Refrigeration, Number 4, Vol 18, p. 220-227, 1995.

[7] Kovacevic, A. and Rane, S. *3D CFD analysis of a twin screw expander*, 8th International Conference on Compressors and their Systems, pp. 417-429, City University London, 9-10 September, 2013.

[8] Paul, C. H. *Compressors Hand Book* McGraw Hill, 2011.

[9] Lujn, J.M., Serrano, J.R., Dolz, V. and Snchez, J. *Model of the expansion process for R245fa in an Organic Rankine Cycle (ORC).* Applied Thermal Engineering, Vol. 40, pp. 248-257, 2012.

[10] Aungier, R. H. *A fast, accurate real gas equation of state for fluid dynamic analysis applications.* Journal of Fluids Engineering, Vol. 117, pp. 277-281, 1995.